Hindawi Publishing Corporation
Mathematical Problems in Engineering
Volume 2012, Article ID 618979, 13 pages
doi:10.1155/2012/618979

Research Article

Intelligent Risk Assessment for Dewatering of Metro-Tunnel Deep Excavations

X. W. Ye,[1] L. Ran,[2] T. H. Yi,[3] and X. B. Dong[2]

[1] *Institute of Transportation Engineering, College of Civil Engineering and Architecture, Zhejiang University, Hangzhou 310058, China*
[2] *Hangzhou Metro Group Co., Ltd., Hangzhou 310020, China*
[3] *Research Center for Structural Health Monitoring and Control, School of Civil Engineering, Dalian University of Technology, Dalian 116023, China*

Correspondence should be addressed to T. H. Yi, yth@dlut.edu.cn

Received 14 October 2012; Accepted 4 November 2012

Academic Editor: Sheng-yong Chen

In recent years, China has been undergoing a metro railway construction boom in order to alleviate the urban traffic congestion problem resulting from the rapid urbanization and population growth in many metropolises. In the construction of metro systems, deep excavations and continuous dewatering for construction of the metro tunnels and stations remain a challenging and high risk task in densely populated urban areas. Intelligent computational methods and techniques have exhibited the exceptional talent in dealing with the complicated problems inherent in the deep excavation and dewatering practice. In this paper, an intelligent risk assessment system for deep excavation dewatering is developed and has been applied in the project of Hangzhou Metro Line 1 which is the first metro line of the urban rapid rail transit system in Hangzhou, China. The specific characteristics and great challenges in deep excavation dewatering of the metro-tunnel airshaft of Hangzhou Metro Line 1 are addressed. A novel design method based on the coupled three-dimensional flow theory for dewatering of the deep excavation is introduced. The modularly designed system for excavation dewatering risk assessment is described, and the field observations in dewatering risk assessment of the airshaft excavation of Hangzhou Metro Line 1 are also presented.

1. Introduction

With the rapid expansion of industrialization and urbanization, traffic congestion has become a serious social problem in most of the large cities in China. Establishment of a large-scale metro network has been recognized to be a most effective way in alleviating the urban traffic congestion problem [1, 2]. In recent years, a large amount of metro railway construction

accompanied by deep excavations in densely populated areas has been undergone in the metropolises of China. For the metro-tunnel excavation to be opened below the groundwater level, a reasonable and robust dewatering system is always desired to obtain the required working condition during the excavation construction period. An effective and efficient dewatering system can be achieved through the integration of groundwater flow modeling, inverse simulation analysis, and optimization formulation to minimize the total amount of water pumpage or implementation cost while satisfying the design criteria [3–5].

It has been well known that the dewatering of the confined aquifer for deep excavations may bring adverse impacts on the surrounding buildings and environments, such as consolidation and compression of the soil layers, settlement and deformation of the piles, cracking and inclination of the buildings, and so forth [6]. Therefore, it becomes essential and desirable to investigate the hydraulic characteristics of deep excavation dewatering as well as the interactions of the underground continuous wall, the seepage well, and the soil layers, which have attracted a great deal of academic and industrial attention from numerous investigators and practitioners worldwide [7–11].

Chen and Xiang [12] proposed a procedure for estimation of dewatering-induced pile settlement through four steps including a pumping model, a simplified consolidation evaluation, a pile-soil interaction model, and a semitheoretical pile settlement prediction. Schroeder et al. [13] presented the practice of planning and execution of dewatering for a deep excavation in coarse alluvium containing cobbles and boulders. Wang et al. [14] developed a decision support system for dewatering systems selection (DSSDSS) for determination of the most appropriate dewatering system for a project. Forth [15] reported the groundwater control for deep excavations and geotechnical aspects in Hong Kong.

Up to now, a set of nature-inspired computational methodologies and approaches, such as artificial neural networks, fuzzy logic systems, genetic algorithms, and so forth, have been developed and are being powerful tools for quantitatively identifying the constitutive parameters and solving the optimization problems in various engineering fields [16–23]. In this study, an intelligent risk assessment system for deep excavation dewatering construction is developed with integration of the novel computational intelligence and has been exemplified to implement dewatering risk assessment of the airshaft excavation of Hangzhou Metro Line 1.

2. Deep Excavation Dewatering of Metro-Tunnel Airshaft

2.1. Metro-Tunnel Airshaft

Hangzhou Metro Line 1 is the first metro line of the urban rapid rail transit system in Hangzhou, China, which is one of the largest municipal projects of Hangzhou and is being constructed starting from 28 March 2007 and will be officially put into operation in the end of October 2012. This metro line has a total length of 48 km and 34 stations, connecting Hangzhou downtown with suburban area of the city. It starts from the south at the Xianghu Station in Xiaoshan District, stretches northwards to the Binjiang Station adjacent to the Qiantang River, crosses beneath the Qiantang River to the Fuchun Road Station, passes through Hangzhou downtown, and ends in the Linping Station, with a branch line ending in Xiasha District which diverges from the main line at the Jiubao Station. The 2nd construction segment of Hangzhou Metro Line 1 covers from the Binjiang Station to the Jiubao Station with a length of 25 km. In this construction section, a two-lane single-bore shield tunnel has

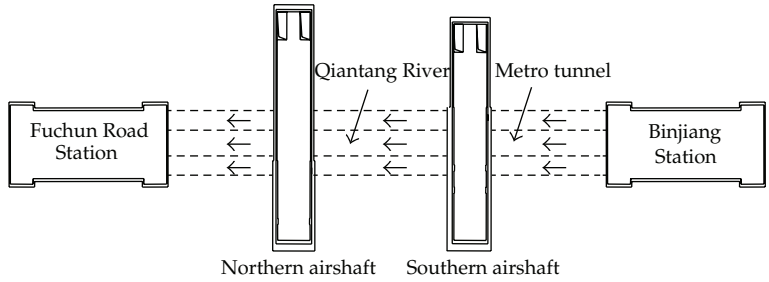

Figure 1: River-crossing metro tunnel and airshafts.

been constructed under the Qiantang River to link the Binjiang Station and the Fuchun Road Station, with two airshafts (the southern airshaft and the northern airshaft) being settled at both sides of the Qiantang River, as illustrated in Figure 1.

2.2. Dewatering of Airshaft Excavation

In this study, the deep excavation and dewatering strategy for the southern airshaft will be addressed. As illustrated in Figure 2, the excavation depth of the southern airshaft is 29.271 m with a planar dimension of 25.4 m × 16.0 m, and the maintenance depth of the southern airshaft excavation is 48.0 m. The deep excavation construction of the southern airshaft excavation contains 15 construction steps, that is, step 1—excavation of the fourth soil layer, step 2—construction of the fourth concrete ring-shape purlin, step 3—construction of the lining wall on the second floor underground, step 4—excavation of the fifth soil layer, step 5—construction of the fifth concrete ring-shape purlin and supporting structures, step 6—construction of the lining wall on the third floor underground, step 7—concrete curing, step 8—excavation of the sixth soil layer, step 9—construction of the sixth concrete ring-shape purlin, step 10—concrete curing, step 11—excavation of the last soil layer, step 12—base-plate pouring, step 13—base-plate curing, step 14—lining pouring, and step 15—capping operation.

With the aid of the static cone penetration tests, the foundation of the southern airshaft can be divided into 20 soil layers in the depth direction. Table 1 lists the hydraulic and mechanical properties of different soil layers of the southern airshaft foundation. Two confined aquifers are distributed in the soil layer $⑥_3$ and the soil layers $(14)_1$ and $(14)_2$, and the groundwater level will be greatly affected by the seasonal variation and the water level of the Qiantang River. The complicated engineering geological and hydrogeological conditions of the southern airshaft foundation bring great challenges in excavation dewatering works. The complexity and high risks in the dewatering process for deep excavation of the southern airshaft are reflected in the following issues: (i) the excavation depth of the southern airshaft excavation is large; (ii) the round gravel layer with a high coefficient of permeability is not deeply buried; (iii) the underground water level is anticipated to be largely descended to meet the designed drawdown requirement; (iv) the southern airshaft excavation is adjacent to the Qiantang River and the hydraulic relationship between the surface water and the underground water is inexplicit; (v) the hydraulic connection between different soil layers of the southern airshaft foundation is not clear.

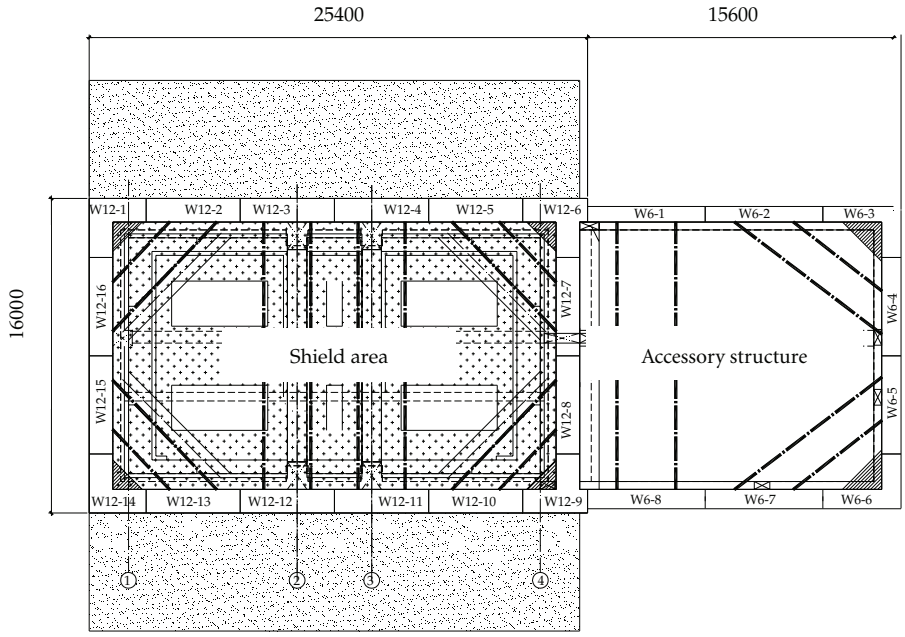

(a) Plan view

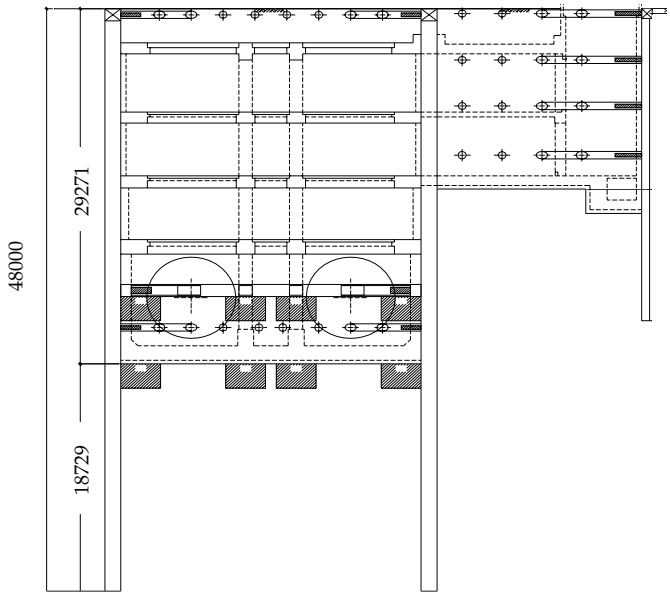

(b) Cross-sectional view

Figure 2: Schematic of southern airshaft excavation (unit: mm).

Table 1: Hydraulic and mechanical properties of soil layers of southern airshaft foundation.

No.	Soil layer	Thickness of soil layer (m)	Coefficient of permeability (cm/s)	Modulus of compressibility (MPa)
①$_1$	Miscellaneous fill soil	0.70 ~ 3.10	5.0E – 03	—
①$_2$	Plain fill soil	0.30 ~ 6.00	8.0E – 04	6.5
③$_1$	Sandy silt	3.4	4.0E – 04	7.0
③$_2$	Sandy silt	3.50 ~ 9.70	7.0E – 04	8.5
③$_4$	Sandy silt	1.00 ~ 5.90	6.5E – 04	5.5
③$_5$	Silty sand and sandy silt	1.60 ~ 7.00	3.0E – 03	7.0
③$_6$	Silt	4.20 ~ 10.95	4.0E – 03	10.0
③$_7$	Sandy silt	0.80 ~ 6.20	2.0E – 04	5.5
③$_8$	Silt	—	4.5E – 03	10.5
④$_3$	Silty soft clay	2.60 ~ 6.70	3.0E – 06	2.6
⑥$_1$	Silty soft clay	1.50 ~ 3.70	2.0E – 06	2.7
⑥$_2$	Silty soft clay	1.00 ~ 8.30	5.0E – 06	2.8
⑥$_3$	Silt	0.50 ~ 3.85	3.0E – 03	8.0
⑧$_2$	Silty soft clay	0.80 ~ 8.20	4.0E – 05	3.0
⑧$_3$	Silty-fine sand	1.80 ~ 8.50	5.0E – 03	8.5
⑩$_1$	Silty clay	1.90 ~ 4.30	8.0E – 06	3.2
⑩$_2$	Silty clay	2.80 ~ 4.60	4.0E – 06	4.5
(14)$_1$	Medium sand	—	6.0E – 03	11.0
(14)$_2$	Rounded pebble	—	3.5E – 01	—

3. Intelligent Dewatering Risk Assessment System

3.1. Novel Design Method of Deep Excavation Dewatering

During the dewatering process of the deep excavation, one of the key problems is how to handle the issue of confined water decompression which is the most critical risk sources in the deep excavation practices. Currently existent design methods for dewatering of the deep excavation are primarily based on the theory of groundwater dynamics and have the following limitations: (i) the existing design methods for dewatering of the deep excavation are originated from the water supply theory and have not sufficiently taken into account the function of the waterproof curtain of the supporting structure; (ii) the empirical equations or the analytical methods are mainly adopted in the existing design methods for dewatering of the deep excavation with the fact of ignoring the detouring flow effect of the underground wall; (iii) both the anisotropic property of the soil layer and the three-dimensional flow effect of the partially penetrating well near the underground wall are neglected in the existing design methods for dewatering of the deep excavation.

For deep excavation construction of the southern airshaft of Hangzhou Metro Line 1, the traditional dewatering method is lack of robustness in fulfilling the targeted drawdown requirement. In this connection, a novel design method based on the coupled three-dimensional flow theory for dewatering of the airshaft excavation is developed in recognition that the implementation of the full waterproof curtain is highly difficult and costly. In the proposed method, the coupling effects amongst the underground continuous wall, the seepage

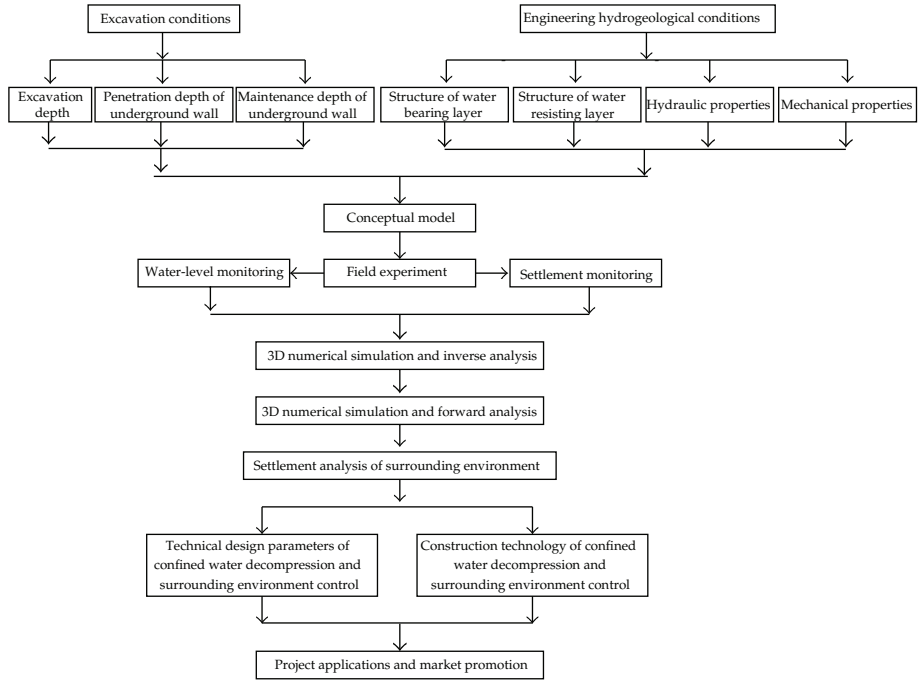

Figure 3: Design and implementation procedure for dewatering of airshaft excavation.

well, and the soil layers are fully taken into account to reach the targets of maximizing the water-level drawdown inside the airshaft excavation and minimizing both the pump output inside the airshaft excavation and the water-level drawdown outside the airshaft excavation. Figure 3 illustrates the basic design and implementation procedure of the proposed method for dewatering of the airshaft excavation.

3.2. Framework of Intelligent Risk Assessment

In recognizing the complexity of dewatering for the confined water in the round gravel layer, an intelligent risk assessment system has been developed to ensure the construction safety during the dewatering process for the southern airshaft excavation. This system is modularly designed and consists of four independent modules: Module 1—Water-level Automatic Collection and Surveillance System (WL-ACSS), Module 2—Water-level Remote Transmission and Assessment System (WL-RTAS), Module 3—Water-level Automated Alarming System (WL-AAS), and Module 4—Auxiliary and Inspection System (AIS). The integration of these four modules is shown in Figure 4.

The WL-ACSS system employs advanced water-level automatic instruments and high-precision vibrating-wire water-level sensors to automatically monitor the underground water-level of the airshaft excavation. It is devised to continuously collect and record the kinetic water-level data for both the observation wells and the pumping wells within a designated time interval. Incorporated with the customized software, the WL-ACSS system is capable of graphically displaying the monitored water-level data and intuitively reflecting the present operational condition of depressurization dewatering. By so doing, the abnormal

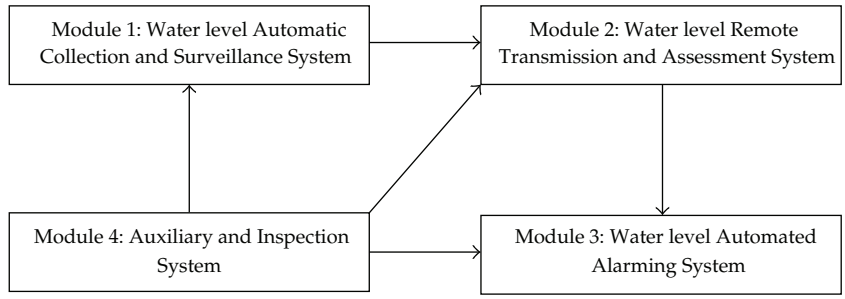

Figure 4: Modular architecture of intelligent risk assessment system.

phenomenon during the dewatering for the airshaft excavation could be readily seized and surveilled in real time to facilitate decision making on timely actions in the event of an emergency.

The WL-RTAS system compiles the monitored water-level data acquired by the WL-ACSS system and generates the specified files suitable for remote transmission through tethered and/or wireless networks. Once the client computers receive the transmitted files, the real-time water-level data will be evaluated with the aid of the coupled three-dimensional flow model which can be expressed by

$$\begin{aligned} \frac{\partial}{\partial x}\left(k_{xx}\frac{\partial h}{\partial x}\right) + \frac{\partial}{\partial y}\left(k_{yy}\frac{\partial h}{\partial y}\right) + \frac{\partial}{\partial z}\left(k_{zz}\frac{\partial h}{\partial z}\right) - W = S_s\frac{\partial h}{\partial t}, \\ k_{xx}\frac{\partial h}{\partial n_x} + k_{yy}\frac{\partial h}{\partial n_y} + k_{zz}\frac{\partial h}{\partial n_z}\bigg|_{\Gamma_2} = q(x,y,z,t), \\ h(x,y,z,t)\big|_{t=t_0} = h_0(x,y,z), \end{aligned} \tag{3.1}$$

where k_{xx}, k_{yy}, and k_{zz} represent the coefficients of permeability in x, y, and z direction, respectively; h is the water head in time t; W is the source/sink term; S_s is the water storage rate; Γ_2 is the boundary condition; n_x, n_y, and n_z denote the unit vectors of the external normal lines along x, y, and z directions, respectively; q is the water recharge per unit area.

The WL-AAS system includes the water-level anomaly alarming system and the power-supply interruption alarming system. For the water-level anomaly alarming system, the warning facilities are allocated at the wellheads and the control room for generating the alarm bumming with light signals. The dynamic variation of the water-level of the airshaft excavation will be tracked and the alarm trigger will be activated once the abnormal water-level is identified by use of a novel threshold detection algorithm. The power-supply interruption alarming system will promptly notify the site managers to inspect or switch the electric circuits when the power goes out.

The AIS system provides the accessory equipment for the intelligent risk assessment system and a laptop-computer-aided portable system for inspecting and maintaining sensors, data acquisition units, and cable networks.

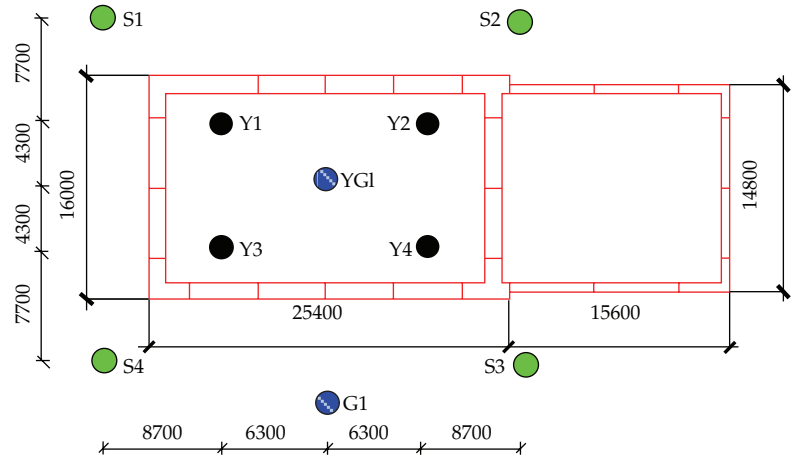

Figure 5: Dewatering wells distributed around southern airshaft excavation (unit: mm).

4. Dewatering Risk Assessment of Airshaft Excavation

4.1. Field Pumping Experiments

After rationally disposing the pumping wells and the observation wells around the region of airshaft excavation, field pumping experiments have been conducted with the purpose of providing sufficient data samples for numerical simulation study of the coupling effect amongst the underground wall, the seepage well, and the soil layers, inferring the hydro-geological parameters of the soil layers and the single-well water flow rate, and validating the hydraulic relationships between different soil layers and the feasibility of confined aquifer dewatering. Figure 5 shows the plan view of the dewatering wells distributed around the excavation area of the southern airshaft. Four pumping wells with a depth of 50 m, that is, Y1, Y2, Y3, and Y4, were allocated inside the southern airshaft excavation; while four pumping wells, that is, S1, S2, S3, and S4 with a depth of 54 m, were deployed outside the southern airshaft excavation. Additionally, two observation wells, that is, YG1 with a depth of 50 m and G1 with a depth of 48 m, were arranged inside the southern airshaft excavation and outside the southern airshaft excavation, respectively.

Multiwell pumping experiments have been carried out for efficiency assessment of the dewatering wells inside the southern airshaft excavation (Y1~Y4) and outside the southern airshaft excavation (S1~S4), respectively. The water-level drawdown of the observation wells (YG1 and G1) has been continuously recorded by the water-level automatic collection system and remotely transmitted to the control room in real time. For the pumping experiments inside the southern airshaft excavation, four pumping wells will be activated in sequence at a time interval of 2 hours and then ceased sequentially at the same time interval; while for the four pumping experiments outside the southern airshaft excavation, the time interval for turn-on and shut-down of the pumping wells is 10 hours.

Figure 6 illustrates the measured water-level drawdown of the two observation wells (YG1 and G1) during multiwell pumping experiments inside the southern airshaft excavation. It is seen from Figure 6 that the water-level of the observation well YG1 which is located inside the southern airshaft excavation declines dramatically when the four pumping wells (Y1~Y4) are enabled gradually. The maximum water-level drawdown of the observation well

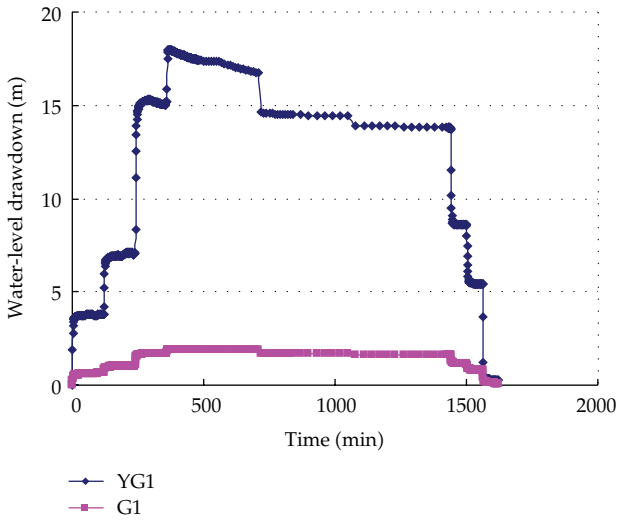

Figure 6: Water-level drawdown of observation wells during multiwell pumping experiments inside southern airshaft excavation.

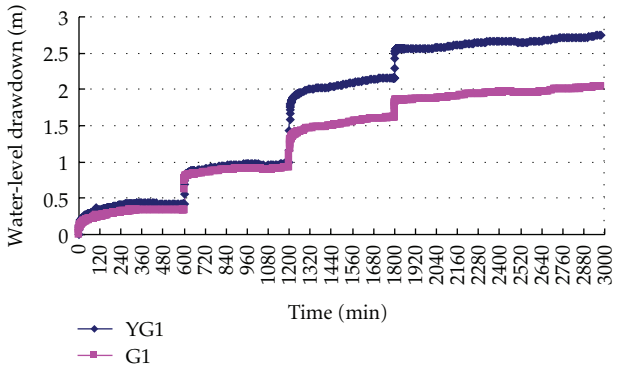

Figure 7: Water-level drawdown of observation wells during multiwell pumping experiments outside southern airshaft excavation.

YG1 reaches 18.00 m which is larger than the targeted water-level drawdown of 11.72 m. On the other hand, the water-level of the observation well G1 outside the southern airshaft excavation declines slowly and the maximum water-level drawdown of the observation well G1 is only 1.92 m. The main reason for the great difference of water-level drawdown between the two observation wells is because the underground continuous wall obstructs the hydraulic connection between the confined aquifers inside and outside the southern airshaft excavation.

Figure 7 shows the measured water-level drawdown of the two observation wells (YG1 and G1) during multiwell pumping experiments outside the southern airshaft excavation. It is observed from Figure 7 that the water-levels of the two observation wells decline almost synchronously. The maximum water-level drawdown of the two observation wells is 2.75 m which is much less than the targeted water-level drawdown of 11.72 m. Therefore,

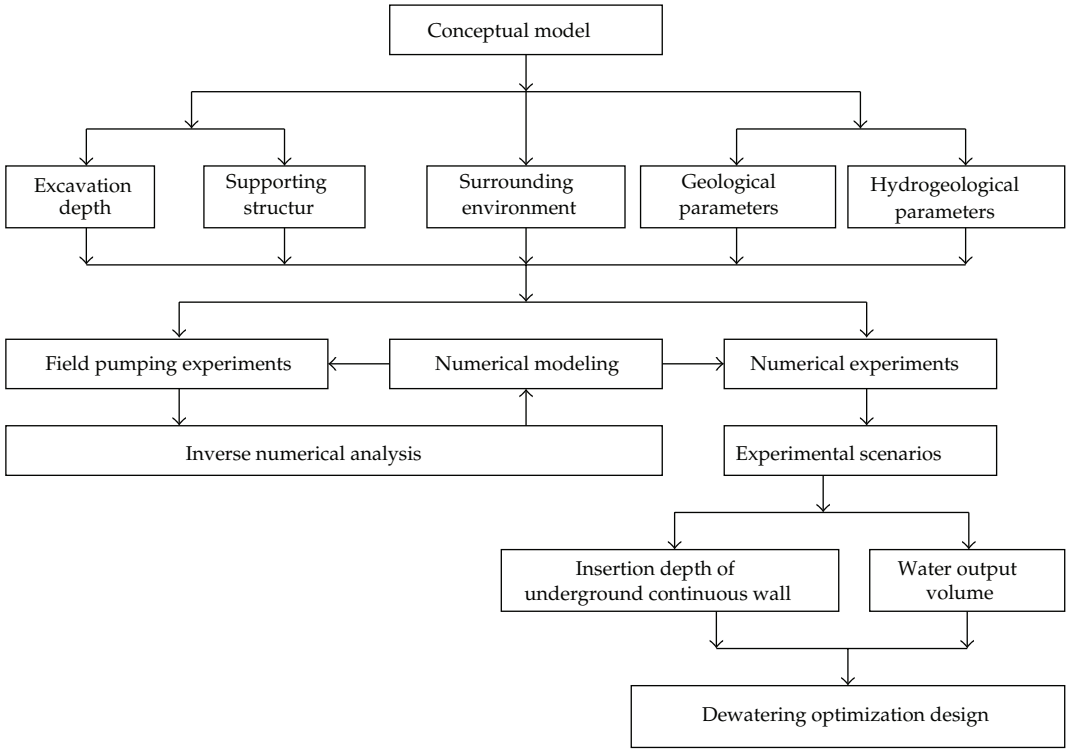

Figure 8: Flowchart of inverse simulation analysis for deep excavation dewatering.

the dewatering scheme by pumping the wells outside the southern airshaft excavation will not be adopted in this project.

4.2. Inverse Simulation and Extrapolation Analysis

Based on the measurement data from the field pumping experiments, the hydraulic parameters of different soil layers are derived by inverse simulation analysis, and then the conceptual model of excavation dewatering will be improved to be a quantitative analytical model for further dewatering efficiency analysis and risk assessment of various scenarios. Meanwhile, with such an updated analytical model, the interaction analysis between the underground continuous wall and the dewatering wall can be executed to facilitate the dewatering optimization design, dewatering mechanism analysis, and dewatering method extrapolation. Figure 8 shows the flowchart of the inverse simulation analysis for dewatering of the airshaft excavation.

Figure 9 shows the calculated water-level drawdown at three different locations, that is, the top of the confined aquifer (YG1-A), the middle of the confined aquifer (YG1-B), and the bottom of the confined aquifer (YG1-C) with the variation of the insertion depth of the underground continuous wall. It is revealed from Figure 9 that with the increasing of the insertion depth of the underground continuous wall, the water-level drawdown will increase gradually for all the three measurement locations. Figure 10 illustrates the predicted water output volume with the variation of the insertion depth of the underground continuous wall

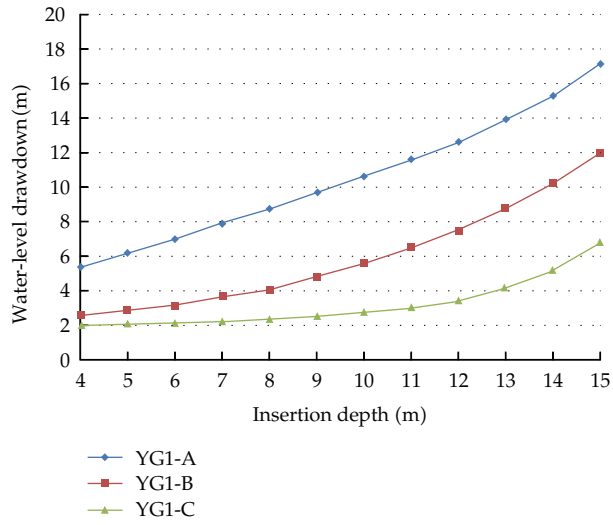

Figure 9: Water-level drawdown versus insertion depth of underground continuous wall.

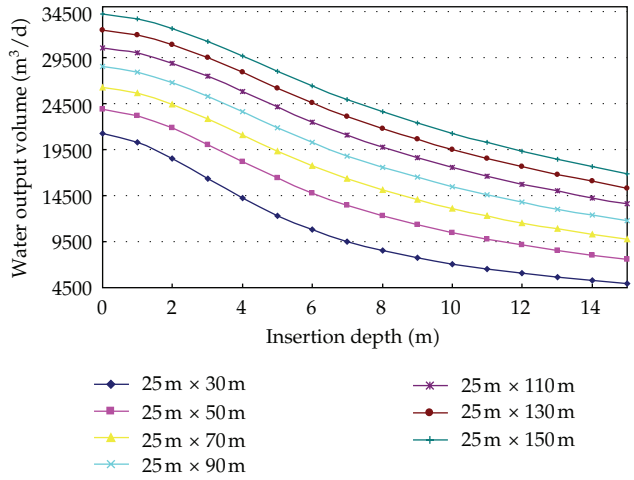

Figure 10: Water output volume versus insertion depth of underground continuous wall.

for different geometrical dimensions of the deep excavation. From Figure 10, it is indicated that the predicted water output volume will decrease gradually with the increasing of the insertion depth of the underground continuous wall. A further observation into Figure 10 reveals that with the increasing of the geometrical dimensions of the deep excavation, the predicted water output volume will increase.

5. Conclusions

The safety of deep excavation dewatering for the metro tunnels and stations has gained great concerns which will bring geological disasters and pose threat to the public safety in metropolitan regions. In recognition of the limitations existent in the traditional dewatering

method, a novel design method for excavation dewatering has been developed on the basis of the coupled three-dimensional flow theory. An intelligent risk assessment system has been developed in modular architecture and applied to evaluate the safety of excavation dewatering for the metro-tunnel airshaft of Hangzhou Metro Line 1.

In this study, the following specific conclusions are drawn: (i) there is a great difference of water-level drawdown between the observation well inside the airshaft excavation and that outside the airshaft excavation during multiwell pumping experiments inside the airshaft excavation; this is because the underground continuous wall obstructs the hydraulic connection between the confined aquifers inside and outside the airshaft excavation; (ii) the water-level drawdown results of the observation wells during multiwell pumping experiments outside the airshaft excavation reveal that the dewatering scheme by pumping the wells outside the airshaft excavation is inappropriate; (iii) with the increasing of the insertion depth of the underground continuous wall, the water-level drawdown will increase gradually while the predicted water output volume will decrease.

Acknowledgments

This research work was jointly supported by the Science Fund for Creative Research Groups of the NSFC (Grant no. 51121005), the National Natural Science Foundation of China (Grant no. 51178083, 51222806), and the Program for New Century Excellent Talents in University (Grant no. NCET-10-0287). The authors also wish to express their thanks to the Hangzhou Metro Group Co., Ltd., for permission to publish this paper.

References

[1] Y. Y. Kim and K. K. Lee, "Disturbance of groundwater table by subway construction in the Seoul area, Korea," *Geosciences Journal*, vol. 7, no. 1, pp. 37–46, 2003.

[2] J. C. Ni and W. C. Cheng, "Shield machine disassembly in grouted soils outside the ventilation shaft: a case history in Taipei Rapid Transit System (TRTS)," *Tunnelling and Underground Space Technology*, vol. 26, no. 2, pp. 435–443, 2011.

[3] M. Tokgoz, K. K. Yilmaz, and H. Yazicigil, "Optimal aquifer dewatering schemes for excavation of collector line," *Journal of Water Resources Planning and Management*, vol. 128, no. 4, pp. 248–261, 2002.

[4] D. Roy and K. E. Robinson, "Surface settlements at a soft soil site due to bedrock dewatering," *Engineering Geology*, vol. 107, no. 3-4, pp. 109–117, 2009.

[5] K. Demirbas, A. B. Altan-Sakarya, and H. Onder, "Optimal dewatering of an excavation site," *Proceedings of the Institution of Civil Engineers. Water Management*, vol. 165, no. 6, pp. 327–337, 2012.

[6] N. Zhou, P. A. Vermeer, R. Lou, Y. Tang, and S. Jiang, "Numerical simulation of deep foundation pit dewatering and optimization of controlling land subsidence," *Engineering Geology*, vol. 114, no. 3-4, pp. 251–260, 2010.

[7] M. Preene and W. Powrie, "Steady-state performance of construction dewatering systems in fine soils," *Geotechnique*, vol. 43, no. 2, pp. 191–205, 1993.

[8] W. Powrie and T. O. L. Roberts, "Case history of a dewatering and recharge system in chalk," *Geotechnique*, vol. 45, no. 4, pp. 599–609, 1995.

[9] C. I. Mansur and S. G. Durrett, "Dewatering cofferdam for construction of Olmsted Locks," *Journal of Geotechnical and Geoenvironmental Engineering*, vol. 128, no. 6, pp. 496–510, 2002.

[10] A. Aryafar and F. D. Ardejani, "Anisotropy and bedding effects on the hydro geological regime in a confined aquifer to design an appropriate dewatering system," *International Journal of Environmental Science and Technology*, vol. 6, no. 4, pp. 563–570, 2009.

[11] M. A. Bevan, W. Powrie, and T. O. L. Roberts, "Influence of large-scale inhomogeneities on a construction dewatering system in chalk," *Geotechnique*, vol. 60, no. 8, pp. 635–649, 2010.

[12] S. Chen and Y. Xiang, "A procedure for theoretical estimation of dewatering-induced pile settlement," *Computers and Geotechnics*, vol. 33, no. 4-5, pp. 278–282, 2006.

[13] W. L. Schroeder, V. W. Rybel, and L. Cochran, "Dewatering for Opal Springs Powerhouse excavation," *Journal of Construction Engineering and Management*, vol. 112, no. 3, pp. 440–451, 1986.
[14] S. Q. Wang, Y. P. Wee, and G. Ofori, "DSSDSS: a decision support system for dewatering systems selection," *Building and Environment*, vol. 37, no. 6, pp. 625–645, 2002.
[15] R. A. Forth, "Groundwater and geotechnical aspects of deep excavations in Hong Kong," *Engineering Geology*, vol. 72, no. 3-4, pp. 253–260, 2004.
[16] C. Rechea, S. Levasseur, and R. Finno, "Inverse analysis techniques for parameter identification in simulation of excavation support systems," *Computers and Geotechnics*, vol. 35, no. 3, pp. 331–345, 2008.
[17] S. Y. Chen and Y. F. Li, "Vision sensor planning for 3-D model acquisition," *IEEE Transactions on Systems, Man, and Cybernetics, Part B*, vol. 35, no. 5, pp. 894–904, 2005.
[18] S. Y. Chen, Y. F. Li, and J. Zhang, "Vision processing for realtime 3-D data acquisition based on coded structured light," *IEEE Transactions on Image Processing*, vol. 17, no. 2, pp. 167–176, 2008.
[19] F. Kang, J. Li, and Q. Xu, "Structural inverse analysis by hybrid simplex artificial bee colony algorithms," *Computers and Structures*, vol. 87, no. 13-14, pp. 861–870, 2009.
[20] Y. Q. Ni, X. W. Ye, and J. M. Ko, "Monitoring-based fatigue reliability assessment of steel bridges: analytical model and application," *Journal of Structural Engineering*, vol. 136, no. 12, pp. 1563–1573, 2010.
[21] S. Y. Chen, "Kalman filter for robot vision: a survey," *IEEE Transactions on Industrial Electronics*, vol. 59, no. 11, pp. 4409–4420, 2012.
[22] S. Y. Chen, H. Tong, and C. Cattani, "Markov models for image labeling," *Mathematical Problems in Engineering*, vol. 2012, Article ID 814356, 18 pages, 2012.
[23] Y. Q. Ni, X. W. Ye, and J. M. Ko, "Modeling of stress spectrum using long-term monitoring data and finite mixture distributions," *Journal of Engineering Mechanics*, vol. 138, no. 2, pp. 175–183, 2012.